LIDS-P-2253

Wavelet-Packet-Based Multiple Access Communication

Rachel E. Learned Hamid Krim Bernhard Claus

Alan S. Willsky W. Clem Karl

Laboratory for Information and Decision Systems
Massachusetts Institute of Technology
Cambridge, MA 02139
email: learned@lids.mit.edu

June 24, 1994

To appear in the Proceedings of the July, 1994, SPIE International Symposium on Optics, Imaging, and Instrumentation – Mathematical Imaging: Wavelet Applications in Signal and Image Processing (2303-20)

ABSTRACT

We explore the role that the wavelet packet transform can play in increasing multiple access communication throughput via waveform design and receiver design. Wavelet packets offer a flexible framework which allows us to select and refine signature waveforms at intermediate time-frequency levels leading to the development of efficient methods for near optimal receiver implementation. The optimal receiver will jointly demodulate all of the received waveforms and has a complexity which is exponential in the number of users, while a suboptimal version will attempt to do the same with a greatly reduced computational complexity. We believe that our wavelet packet recursive joint detection system described in this paper offers a good alternative approach to existing comparable methods. Specifically, our preliminary analysis and simulation results indicate the potential for a marked computational improvement over the optimal detector and additional flexibility and efficiency over other proposed joint detection schemes for multiple access communication.

KEY WORDS: joint detection, multiple access communication, mutli-user communication, wavelet packets

1 INTRODUCTION

Multiple access (MA) communication, in which a common medium is shared by many users, has recently re-emerged as an active area of research. The primary goal of a MA system design is to maximize the overall throughput (often, this translates to maximizing the number of users). By allowing many users to transmit simultaneously in the same frequency band, we are inducing interference among users. This inter-user or multiple access interference (MAI) will degrade the performance of conventional receivers which treat the MAI as white

Gaussian noise and detect the user of interest as a single user. At high signal to noise ratios, MAI is the primary limiting factor for systems supporting a large number of users.

The performance of a MA system is greatly enhanced by jointly decoding the transmissions of all the users as opposed to treating them as white Gaussian noise [1]. In the current literature, much attention is focused on overcoming the MAI effects, but the signal design aspect and the receiver design aspect of the MA system are always considered separately. The prior investigations of joint detection have concentrated on receiver design and are in principle applicable to any signal set.[1] Performance and receiver complexity, on the other hand, depend crucially on the signal set structure. Wedding signal design to receiver development leads to interesting and challenging problems.

The objective of this work is to explore the role that the wavelet packet transform (WPT) can play in the design of MA joint detection systems. Wavelet packets offer a flexible framework which allows us to select and refine signature waveforms at intermediate time-frequency levels and to develop efficient methods for receiver implementation. In this paper, we use the structure of the WPT to choose signal sets *and* design the receiver to obtain an efficient MA system. We take advantage of the hierarchical nature of our wavelet packet signal sets to control multiple access interference providing structure that can be exploited in receiver design. In particular, we describe a method for designing wavelet-packet-based multiple access waveforms and we develop and analyze a wavelet-packet-based recursive demodulation scheme that follows from the waveform structures.

Our MA scenario for this paper is as follows:

- The user waveforms are known exactly, including their relative time shifts.
- Antipodal signaling is used, i.e. we modulate the user waveform with 1 to represent a bit of 1 and with -1 to represent a bit of 0.
- We observe our system for a single block of time and assume that any transmissions in past and future time blocks do not interfere.
- The signals travel through a simple additive white Gaussian noise channel. Multi-path and nonlinear channel effects are addressed elsewhere.
- At the receiver, all users' transmissions appear at the same power.

The resulting received signal, denoted by $\mathbf{r}$, can be written as

$$\mathbf{r} = \sum_{k=1}^{K} b_k \mathbf{w}_k + \sigma \mathbf{n} = \mathbf{W}\mathbf{b} + \sigma \mathbf{n}, \tag{1}$$

where K is the total number of users, b_k is either a 1 or -1 corresponding to a 1 or 0 information bit of the k^{th} user, and $\mathbf{w}_k$ is the k^{th} user's discrete waveform represented as a column vector[2]. The signal power $\mathbf{w}_k^T \mathbf{w}_k = 1$, the bit vector $\mathbf{b} = [b_1\ b_2 \cdots b_K]^T$, and the waveform matrix $W = [\mathbf{w}_1\ \mathbf{w}_2 \cdots \mathbf{w}_K]$. The noise vector, $\mathbf{n}$, is a zero mean, Gaussian random vector with the identity covariance matrix, and σ is the noise level (σ^2 is the noise power).

The matched filter based detector is the result of maximum likelihood detection for the vector $\mathbf{b}$ only if the signals of other users are orthogonal to the signal of interest. Two examples of orthogonal MA schemes are frequency division (FDMA) and time division (TDMA) multiple access, wherein each user is given a non-overlapping frequency or time slot for transmission, respectively. Conventionally, the combined MAI effect of

[1] Often, the signal design aspect of MA is restricted to a general attempt at minimizing correlation among user waveforms.

[2] We assume that all relative time shifts are known and incorporated in $\mathbf{w}_k$.

many nonorthogonal users is viewed as normal white noise and a simple matched filter is used,

$$\hat{b}_k = sgn[\mathbf{w}_k^T \mathbf{r}], \tag{2}$$

where *sgn* represents the signum functional, and $\hat{b}_k$ denotes the estimated bit of the k_{th} user. By assuming the MAI to be white Gaussian noise, we raise the noise level with every user that we add to our scenario. When we treat users as white noise, a large number of users translates to a high noise level, which, in turn, limits throughput.

The MAI, not being an additive white Gaussian noise process[3], has a great degree of structure which can be exploited to lead to other more complex solutions which will afford a relatively larger number of users successful utilization of an MA system. Adopting the optimal approach, i.e. jointly demodulate *all* users, we account for the MAI instead of treating it as additive white Gaussian noise. The maximum likelihood procedure results in the following detector [2]:

$$\hat{\mathbf{b}} = \arg\,[\max_{\mathbf{b}\in\{1,-1\}^K} 2\mathbf{r}^T W\mathbf{b} - (W\mathbf{b})^T W\mathbf{b}\,]. \tag{3}$$

This maximization is over 2^K possible $\mathbf{b}$ vectors (a computational complexity that is exponential in K, the number of users). This optimal method offers substantially higher performance than the conventional demodulator [2], but is impractical for systems having a large number of users because, for large K, the computational burden is immense.

Recent communication literature addresses the general notion of *suboptimal* joint detection which offers, with minimal performance loss, computational simplicity relative to the optimal methods while achieving a significant improvement over the conventional detector [3–5]. These approaches only address the receiver design. The convergence, performance, and receiver complexity of such suboptimal MA detectors, however, crucially depend upon the signal set structure. In light of this, our work in MA systems couples detection and waveform design.

Our method for waveform design takes full advantage of the hierarchical nature of the WPT to minimize MAI by providing structure that can be exploited in receiver design. We have found that our wavelet packet based method for signature waveform design and detector design results in recursive bit estimation procedures similar to those in the recent literature with an overall improvement. Our waveforms possess a nested-type of correlation relationship. This type of correlation structure is extremely well suited for recursive bit estimation. In fact, simply by using our partially correlated wavelet packet derived signature waveforms instead of using partially correlated direct sequence spread spectrum waveforms, immediate possibilities for reduction in computational complexity of other proposed detectors result.

In Section 2 we describe our methodology for waveform design. In Section 3, we develop a general recursive bit estimation procedure and we apply it to our wavelet packet derived user waveforms. We report the findings of several simulations using our wavelet packet signal set and our recursive joint detector in Section 4. Our future work is discussed in Section 5 and our conclusion is in Section 6.

2 WAVELET PACKET USER CONSTELLATIONS

One can view the wavelet packet transform as a tool which allows for seamless transition from TDMA ideas to FDMA ideas. The wavelet packet domain, as we shall see, allows for simple visualization of both the correlation among user waveforms and the interaction of the user bit estimates resulting from suboptimal recursive joint detection. We may begin to understand the great flexibility of our MA signal-set/receiver-design approach through an intuitive explanation of the time-frequency flexibility offered by the wavelet packet transform.

[3] For example, the orthogonality assumption for an FDMA or TDMA system is often not strictly true for any of the following reasons: there are more users than available orthogonal frequency slots or time slots; signals cannot be synchronized to retain orthogonality; etc..

The full wavelet packet transform can be calculated by successive applications of lowpass-downsample and highpass-downsample operations on the time domain signal. As an example, let us step through the calculation of the full wavelet packet transform of the signals shown in Figures 1-a and c, a Dirac delta and two sinusoids, respectively. Figures 1-b and d display the full wavelet packet transforms of these signals. For ease of display, we show the magnitude of the wavelet packet coefficients in each bin, where black corresponds to the highest value and white to zero. The top bin of the full wavelet packet transform contains the time domain signal. The signal representation at level 1 is completely time-resolved. Level 2 of the decomposition contains two bins. The left-most (right-most) bin displays the vector which is obtained by a lowpass-downsample (highpass-downsample) operation on the time domain signal, where the highpass and lowpass filters are quadrature mirror counterparts. Hence, the representation at level 2 of the full wavelet packet transform of a signal contains the same information that exists in the time domain signal at level 1. The level 2 representation has two degrees of frequency resolution, i.e., the low and high frequency portions of the signal have been separated into two bins, but, due to the down sampling, each bin has only half the time resolution that exists at level 1. As we proceed through the levels of the wavelet packet transform, we see a tradeoff between time resolution and frequency resolution. This tradeoff is apparent in the decomposition of our Dirac delta and of our two sinusoids. For the Dirac delta, the representation at the successive levels becomes more diffuse with each level. For the sinusoids, with each successive level, we see a focusing of information into fewer and fewer wavelet packet coefficients. It may be clear, now, that the lowest level of the decomposition offers maximum frequency resolution and no time resolution. The lowest levels of Figures 1-b and d are in close agreement with the discrete Fourier transforms of the Dirac delta and the two sinusoids.[4]

We further illustrate this time-frequency resolution tradeoff by comparing the wavelet packet transforms shown in Figure 1-b, d and f: the Dirac delta (perfectly time resolved), the sinusoids (perfectly frequency resolved), and a time-frequency localized signal (intermediate resolution). Notice that the time-frequency localized signal is most compactly represented at the fourth level of its wavelet packet transform. Through this comparison we wish to convey the many degrees of flexibility that arise when one is not limited to the time domain or frequency domain, but is allowed to analyze and design waveforms which focus at intermediate time/frequency levels.

2.1 The Wavelet Packet Transform

Let $\mathcal{W}(\mathbf{x})$ denote the discrete orthonormal wavelet packet transform of a vector (or discrete signal) $\mathbf{x}$. We call the wavelet packet transform display grid the *tableau*. The bin locations within a tableau will be represented by the bin index (l, c) where l corresponds to the level and c corresponds to the bin number at that level, e.g. bin (l, c) is at level l, c bins from the left. The tableau and our indexing procedure are illustrated in Figure 2. We may write $\mathcal{W}_{(l,c)}(\mathbf{x})$ to denote the bin vector which resides at bin (l, c) of the wavelet packet transform of $\mathbf{x}$.

For completeness, we recall the rudimentary elements of the wavelet packet transform necessary for the later development of our signal design procedure. The interested reader should consult the excellent paper by Coifman and Wickerhauser [6] for a more detailed explanation of wavelet packets. We may calculate each bin vector of $\mathcal{W}(\mathbf{x})$ by pre-multiplying $\mathbf{x}$ by an appropriate ordering of lowpass-downsample and highpass-downsample matrices. In agreement with the majority of the wavelet literature, we denote the lowpass-downsample matrix as H_l and its quadrature mirror counterpart highpass-downsample matrix as G_l. These matrices differ in size at each level to incorporate the change in length of the bin vectors, hence, we subscript the matrices with the appropriate level upon which they may be used. Specifically,

$$\mathcal{W}_{(l+1,2c-1)}(\mathbf{x}) = H_l \mathcal{W}_{(l,c)}(\mathbf{x}) \tag{4}$$

[4] An intuitively pleasing way to view the wavelet packet decomposition tree is to display the bins at a given level so that they occur in increasing frequency order from left to right. The method of decomposition described above results in aliasing which exchanges the frequency ordering of some branches of the tree. A simple swapping of the appropriate bins corrects the problem. Figure 1 is the only figure in this paper that reflects the re-ordering of the wavelet packet transform display.

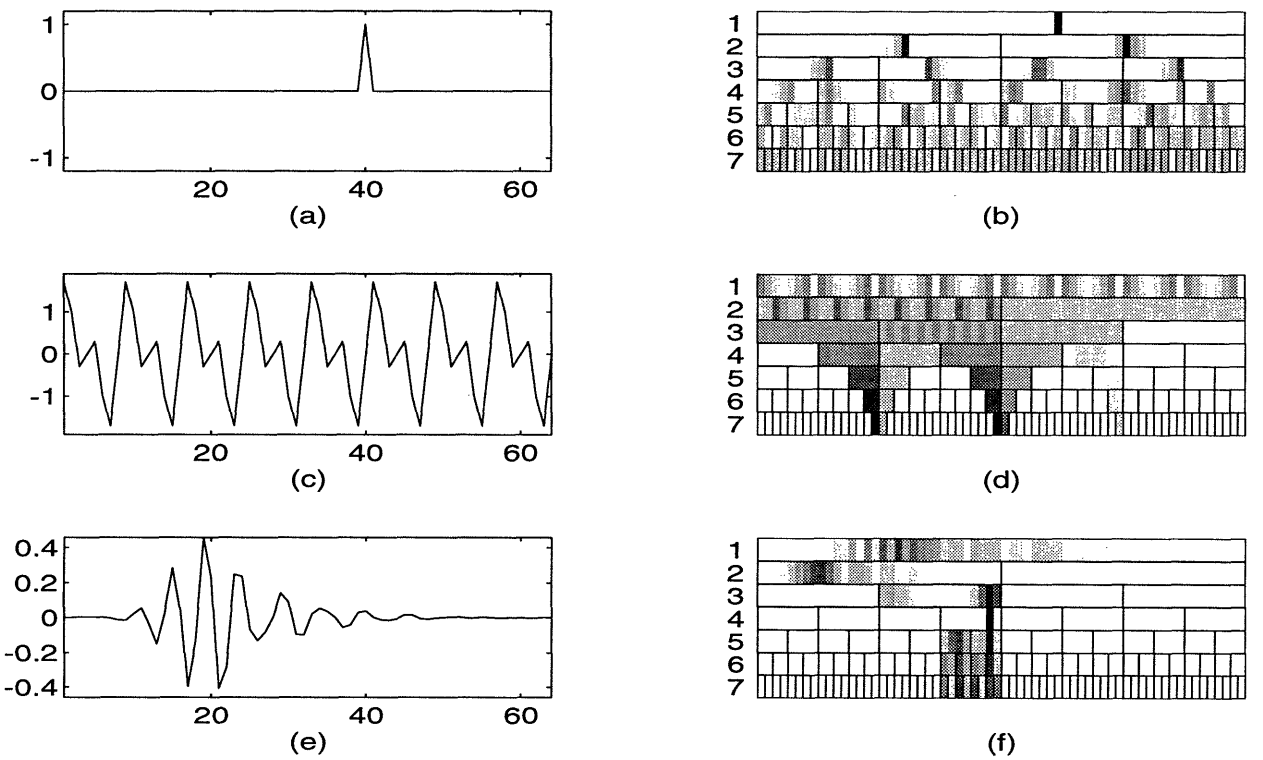

Figure 1: a) An impulse in time. b) Full WPT of the impulse. c) Two sinusoids. d) Full WPT of the sinusoids. e) A time and frequency localized signal. f) Full WPT of the time and frequency localized signal.

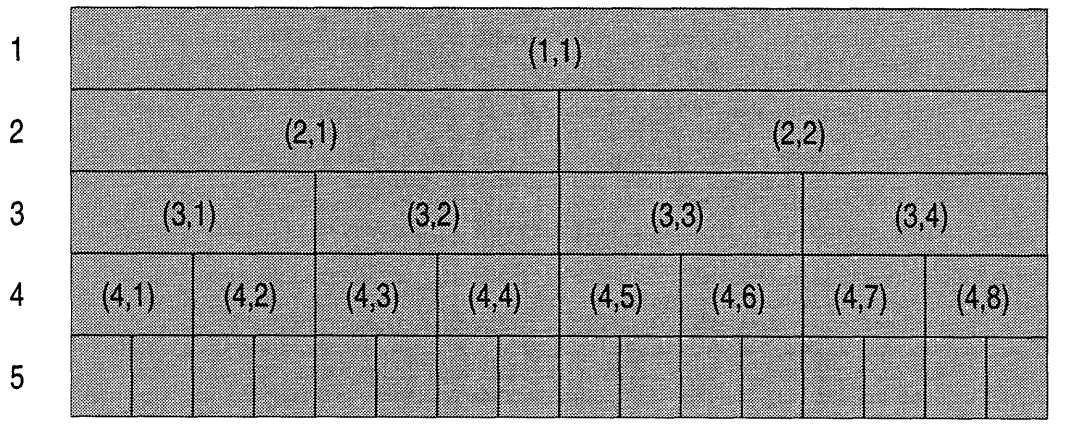

Figure 2: The wavelet packet tableau with indices shown at each bin of the first four levels.

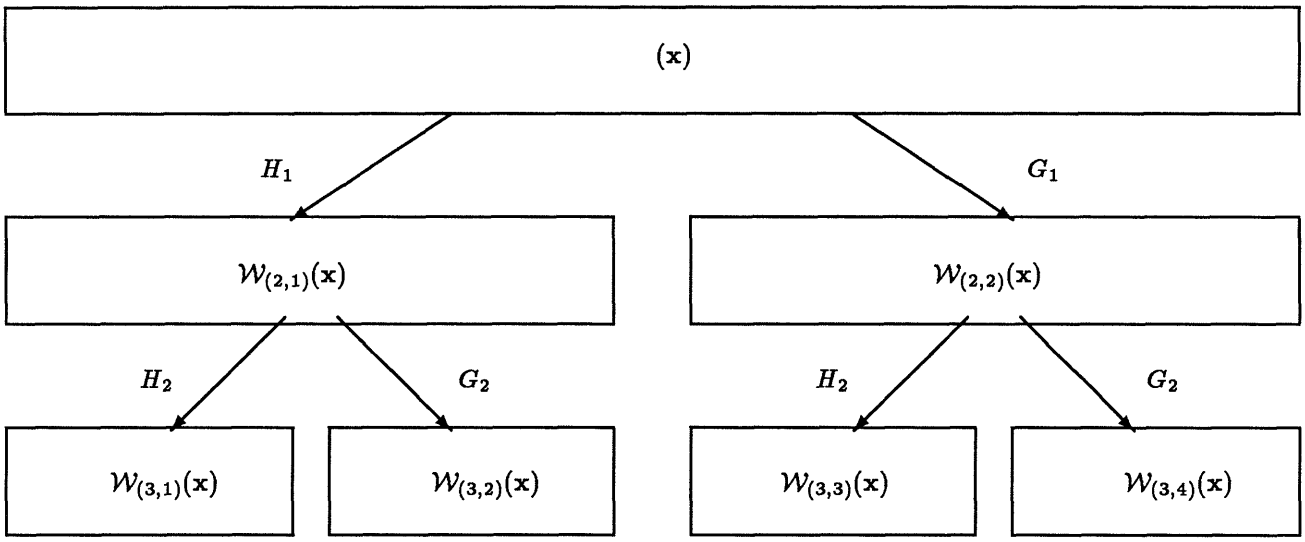

Figure 3: Pictorial representation of the wavelet packet transform of a vector $\mathbf{x}$.

and

$$\mathcal{W}_{(l+1,2c)}(\mathbf{x}) = G_l \mathcal{W}_{(l,c)}(\mathbf{x}). \tag{5}$$

Figure 3 pictorially illustrates the wavelet packet decomposition of a vector $\mathbf{x}$.

We may also calculate a bin vector from its two children bin vectors.

$$\mathcal{W}_{(l,c)}(\mathbf{x}) = H_l^T \mathcal{W}_{(l+1,2c-1)}(\mathbf{x}) + G_l^T \mathcal{W}_{(l+1,2c)}(\mathbf{x}) \tag{6}$$

Some defining properties of the H_l and G_l operators used to calculate the orthonormal wavelet packet transform follow.

$$H_l H_l^T = G_l G_l^T = I \tag{7}$$

$$H_l G_l^T = G_l H_l^T = 0. \tag{8}$$

$$H_l^T H_l + G_l^T G_l = I \tag{9}$$

According to Equation (9), a signal may be *constructed* by working our way back up the tree, applying the appropriate transpose matrices at each step. The signal shown in Figure 1-e was constructed by using the eight bins at level 4 of our tableau, where bin (4,4) is the only one containing a nonzero vector. For this construction, we set the bin vector equal to a unit vector having only one nonzero element. In general, we use $\omega^{\tau}_{(l,c)}$ to denote the unit vector in bin (l, c), having the τ^{th} element equal to 1. To calculate, for instance, the time domain vector $\mathbf{w}^7_{(4,4)}$ from $\omega^7_{(4,4)}$, we have

$$\omega^7_{(4,4)} = [0\,0\,0\,0\,0\,0\,1\,0]^T, \tag{10}$$

and

$$\mathbf{w}^7_{(4,4)} = H_1^T\, G_2^T\, G_3^T\, \omega^7_{(4,4)}. \tag{11}$$

This method of waveform construction has some noteworthy attributes. As seen from the above example, we may create a waveform $\mathbf{w}^{\tau}_{(l,c)}$ from $\omega^{\tau}_{(l,c)}$ for any (l, c) bin of the tableau. We say that the wavelet packet transform of the waveform $\mathbf{w}^{\tau}_{(l,c)}$ *focuses* in bin (l, c) because all non-ancestor and non-descendant bins of (l, c) contain only zeros, and the bin vector in (l, c) contains the most focused (least spread) signal relative to its ancestor and descendant bins. This can be seen in Figure 1-f.

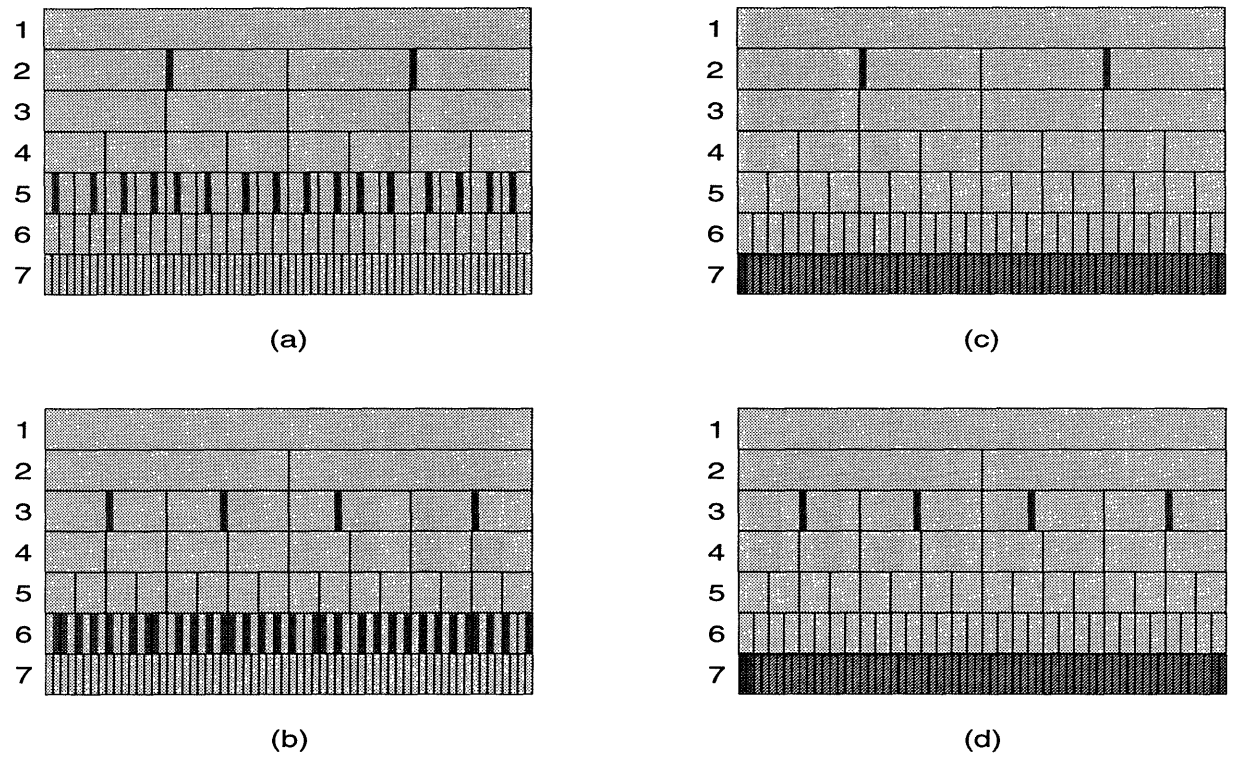

Figure 4: (a) The 5-2 constellation (b) The 6-3 constellation, (c) The 7-2 constellation, (d) The 7-3 constellation

2.2 WPMA Signature Waveforms and the Wavelet Packet User Constellation

In our wavelet packet multiple access (WPMA) system each user is assigned a wavelet-packet-derived waveform; the k^{th} user's waveform is $\mathbf{w}^{\tau}_{(l_k,c_k)}$ as described in the previous section, with $k = 1, \cdots K$. We say that user k is *located* at bin (l_k, c_k).[5] We will use the term *user constellation* to refer to the set of user locations, $\{(l_k, c_k)\}_1^K$.

In this paper we use several two-level constellations which we term the **p-q constellation.** We assign one user to each of the bins at levels p and q of the tableau. We graphically depict any constellation by displaying the user locations via the bin vectors, $\omega_{(l_k,c_k)}$, which were used to construct each of the $k = 1, 2, \cdots, K$ user waveforms. We have arbitrarily chosen our signal length to be 64 samples. For a 64 sample signal, the complete wavelet packet transform contains 7 levels. Figure 4 shows various p-q user constellations.

The received signal resulting from use of the 6-3 WPMA user constellation shown in Figure 4-b for 36 users is

$$\mathbf{r} = \sum_{c=1}^{4} b_{3,c}\mathbf{w}_{(3,c)} + \sum_{c=1}^{32} b_{6,c}\mathbf{w}_{(6,c)} + \sigma\mathbf{n}, \tag{12}$$

where we have simply re-stated Equation (1) substituting the wavelet packet functions for the user signature waveforms.

[5] It is not necessary for us to specify the fixed position, τ, of the non-zero element for our analysis in this paper. The user constellation tableau reflects the τ for each user.

3 WAVELET PACKET RECURSIVE JOINT DETECTION

3.1 Derivation of the Recursive Joint Detector

In the MA scenario described in Section 1, we observe the signal

$$\mathbf{r} = \mathbf{W}\mathbf{b} + \sigma\mathbf{n}. \tag{13}$$

We wish to derive a recursive algorithm to estimate $\mathbf{b}$. We know that $\hat{\mathbf{b}} \in \{1, -1\}^K$ and we use the first estimate resulting from the matched filter output.

$$\hat{\mathbf{b}}(1) = sgn[\mathbf{W}^T\mathbf{r}] \tag{14}$$

Without noise, i.e. $\sigma = 0$, we have $\mathbf{r} = \mathbf{W}\mathbf{b}$ and our first estimate would be

$$\hat{\mathbf{b}}(1) = sgn[\mathbf{W}^T\mathbf{W}\mathbf{b}]. \tag{15}$$

The true bit vector, $\mathbf{b}$, should be a fixed point[6] of our recursion. In general, $\mathbf{b} \neq \mathbf{W}^T\mathbf{W}\mathbf{b}$ so we must add $(\mathbf{b} - \mathbf{W}^T\mathbf{W}\mathbf{b})$ to the argument of Equation (14) so that, in the noiseless case, we have

$$\mathbf{b} = sgn[\mathbf{W}^T\mathbf{W}\mathbf{b} + \mathbf{b} - \mathbf{W}^T\mathbf{W}\mathbf{b}]. \tag{16}$$

This leads to our recursive detector

$$\hat{\mathbf{b}}(m+1) = sgn[\mathbf{W}^T\mathbf{r} + \hat{\mathbf{b}}(m) - \mathbf{W}^T\mathbf{W}\hat{\mathbf{b}}(m)], \tag{17}$$

where $\hat{\mathbf{b}}(0) = 0$ so that Equation (17) reduces to the matched filter estimate for $\hat{\mathbf{b}}(1)$.

We offer a simple interpretation of our joint detector by looking at Equation (17) for noiseless reception, $\mathbf{r} = \mathbf{W}\mathbf{b}$,

$$\hat{\mathbf{b}}(m+1) = sgn[\hat{\mathbf{b}}(m) + \mathbf{W}^T\mathbf{W}(\mathbf{b} - \hat{\mathbf{b}}(m))]. \tag{18}$$

At each recursion, we update the previous estimate with a correction term which is based on the difference between the actual bit vector and the previous bit estimate.

The joint detection procedure defined by Equation (17) is, in fact, equivalent to the recursion proposed by Varanasi and Aazhang [3]. Their derivation is based upon the optimal maximum likelihood solution of Equation (3). They propose the following logical recursive version of Equation (3).

$$\hat{b}_k(m+1) = \arg[\max_{b_k \in \{1,-1\}} 2\mathbf{r}^T\mathbf{W}\tilde{\mathbf{b}}^m(b_k) - (\mathbf{W}\tilde{\mathbf{b}}^m(b_k))^T\mathbf{W}\tilde{\mathbf{b}}^m(b_k)], \tag{19}$$

where $\tilde{\mathbf{b}}^m(b_k) = [\hat{b}_1(m)\ \hat{b}_2(m)\cdots\hat{b}_{k-1}(m)\ b_k\ \hat{b}_{k+1}(m)\cdots\hat{b}_K(m)]^T$ and with $\hat{b}_k(0) = 0$. By expanding Equation (19) into its $\hat{\mathbf{b}}_j(m)$ and b_k components, it is clear that we must choose $\hat{b}_k(m+1)$ according to

$$\hat{b}_k(m+1) = sgn[\mathbf{r}^T\mathbf{w}_k - \sum_{j \neq k} \mathbf{w}_k^T\mathbf{w}_j\hat{b}_j(m)]. \tag{20}$$

It is clear that Equation (20) is equivalent to Equation (17), the result of our derivation.

[6] By fixed point we mean $\hat{\mathbf{b}}(m) = \hat{\mathbf{b}}(m+1) = \mathbf{b}$.

3.2 WPMA Waveforms and the Recursive Joint Detector

We cast the recursive detector into the wavelet packet domain so that we may become familiar with the ways in which users interact with one another. We wish to gain insight for the design of WPMA systems and exploit the properties of these waveforms to develop a fast and near optimal receiver based on the recursive joint detector derived previously.

Recall that the wavelet packet transform of our functions focuses at a single bin with zero vectors in all non-ancestor and non-descendant bins. In tableau terms, interfering users have common descendant bins. Users who do not share descendants are orthogonal. We conclude that many users in a WPMA system will be orthogonal and will not interfere with one another. This allows for us to collect members of a user constellation into *groups*, where a group comprises all users that are related as parent-descendants. Hence, we may eliminate all non-group users from our joint detection algorithm and realize an immediate improvement in computational efficiency.

We illustrate the above discussion through a specific example. In the 6-3 WPMA constellation shown in Figure 4-b, we may form 4 groups comprising users located in the following bins:

- group 1: bin (3,1) and bins (6,c) for $c = 1, \cdots, 8$, (bin (3,1) and the eight level-6 bins that are below it).
- group 2: bin (3,2) and bins (6,c) for $c = 9, \cdots, 16$, (bin (3,2) and the eight level-6 bins below it).
- group 3: bin (3,3) and bins (6,c) for $c = 17, \cdots, 24$, (bin (3,3) and the eight level-6 bins below it).
- group 4: bin (3,4) and bins (6,c) for $c = 25, \cdots, 32$, (bin (3,4) and the eight level-6 bins below it).

This natural separation of users into groups can also be seen by taking the wavelet packet transform of Equation (12). First, we calculate the level 6 bin vectors of $\mathcal{W}(\mathbf{r})$,[7]

$$\mathcal{W}_{(6,i)}(\mathbf{r}) = \sum_{c=1}^{4} b_{3,c}\mathcal{W}_{(6,i)}(\mathbf{w}_{(3,c)}) + \sum_{c=1}^{32} b_{6,c}\mathcal{W}_{(6,i)}(\mathbf{w}_{(6,c)}) + \sigma\mathcal{W}_{(6,i)}(\mathbf{n}) \ , \ i = 1, \cdots, 32. \tag{21}$$

Next, we calculate the level 3 bin vectors,

$$\mathcal{W}_{(3,i)}(\mathbf{r}) = \sum_{c=1}^{4} b_{3,c}\mathcal{W}_{(3,i)}(\mathbf{w}_{(3,c)}) + \sum_{c=1}^{32} b_{6,c}\mathcal{W}_{(3,i)}(\mathbf{w}_{(6,c)}) + \sigma\mathcal{W}_{(3,i)}(\mathbf{n}) \ , \ i = 1, \cdots, 4. \tag{22}$$

By expanding the wavelet packet decomposition as in Equations (4) and (5) and writing the waveforms as in Equation (11) we may take advantage of the properties shown in Equations (7) and (8) to eliminate all non-group users from Equations (21) and (22). For ease of notation, we rewrite (21) and (22) for group 1 users only.

$$\mathcal{W}_{(6,i)}(\mathbf{r}) = b_{3,1}\mathcal{W}_{(6,i)}(\mathbf{w}_{(3,1)}) + b_{6,i}\omega_{(6,i)} + \sigma\mathcal{W}_{(6,i)}(\mathbf{n}) \ , \ i = 1, \cdots, 8. \tag{23}$$

$$\mathcal{W}_{(3,1)}(\mathbf{r}) = b_{3,1}\omega_{(3,1)} + \sum_{c=1}^{8} b_{6,c}\mathcal{W}_{(3,1)}(\mathbf{w}_{(6,c)}) + \sigma\mathcal{W}_{(3,1)}(\mathbf{n}) \ . \tag{24}$$

We see from Equations (23) and (24) that each user at level 6 has only one interferer, namely, the user which is located above it in level 3, while each user at level 3 has eight interferes. With our understanding of the wavelet packet transform, we can also conclude this by looking at the 6-3 constellation.

[7] Recall that the wavelet packet transformation is a linear operation.

The recursive detector for a group 1 user would have two parts

$$\hat{b}_{(6,i)}(m+1) = sgn[\mathcal{W}_{(6,i)}(\mathbf{r})^T \omega_{(6,i)} - \mathcal{W}_{(6,i)}(\mathbf{w}_{(3,1)})^T \omega_{(6,i)} \hat{b}_{(3,1)}(m)] \ , \ i = 1, \cdots, 8 \tag{25}$$

$$\hat{b}_{(3,1)}(m+1) = sgn[\mathcal{W}_{(3,1)}(\mathbf{r})^T \omega_{(3,1)} - \sum_{c=1}^{8} \mathcal{W}_{(3,1)}(\mathbf{w}_{(6,c)})^T \omega_{(3,1)} \hat{b}_{(6,c)}(m)]. \tag{26}$$

Writing the transform as in Equations (4) and (5) and the waveform as in Equation (11) gives us the following equalities: $\mathcal{W}_{(6,i)}(\mathbf{r})^T \omega_{(6,i)} = \mathbf{r}^T \mathbf{w}_{(6,i)}$ and $\mathcal{W}_{(6,i)}(\mathbf{w}_{(3,1)})^T \omega_{(6,i)} = \mathbf{w}_{(3,1)}{}^T \mathbf{w}_{(6,i)}$. We may rewrite Equations (25) and (26) as

$$\hat{b}_{(6,i)}(m+1) = sgn[\mathbf{r}^T \mathbf{w}_{(6,i)} - \mathbf{w}_{(3,1)}{}^T \mathbf{w}_{(6,i)} \hat{b}_{(3,1)}] \ , \ i = 1, \cdots, 8, \tag{27}$$

$$\hat{b}_{(3,1)}(m+1) = sgn[\mathbf{r}^T \mathbf{w}_{(3,1)} - \sum_{c=1}^{8} \mathbf{w}_{(6,c)}{}^T \mathbf{w}_{(3,1)} \hat{b}_{(6,c)}]. \tag{28}$$

Commonly, MA systems employ asynchronous direct sequence spread spectrum (DSSS) user waveforms where any single user experiences interference from all other users.[8] We make two observations: 1) when $\mathbf{w}_k$ is a DSSS waveform, $\mathbf{w}_k^T \mathbf{w}_j$ is, in general, nonzero for all values of j and k, therefore, Equation (17) must decode the bits of all K users to detect a single user's bit; 2) each user experiences the same degree of MAI. In contrast: 1) each of our WPMA waveforms, $\mathbf{w}_{(l_k,c_k)}$, is correlated with only a fraction of the signal set; 2) each user experiences a different degree of MAI. We immediately see that our waveforms offer two advantages in a joint detection MA system: 1) as illustrated above, due to the reduction in the number of correlated users, a large degree of computational simplification is realized [9]; 2) the hierarchical structure of MAI experienced by each user lends itself to the recursive nature of our algorithm.

In light of the above discussion, we expect to develop better recursive joint detectors by designing user sets in which each user experiences a different degree of MAI and by developing a recursive joint detection algorithm that exploits the hierarchical correlation structure. It follows that our joint detector should first estimate the bits corresponding to low MAI users, then, using these estimates, strip away much of the MAI before estimating the bits corresponding to high MAI users. The next section shows the results of simulations of our WPMA joint detection system using the p-q constellations and the detector in Equation (17).

4 SIMULATIONS AND RESULTS

Given the complexity of obtaining a closed form solution for the probability of bit error (PBE) for a MA system which uses recursive joint detection, convention is to obtain a PBE bound. In this paper, we prefer to measure the performance of our WPMA joint detection systems relative to the same WPMA systems using a matched filter detector through bit error rate (BER) curves obtained from Monte-Carlo simulations.[10]

The constellations used for these simulations are of the type shown in Figure 4. We have arbitrarily chosen the bit duration, T_b, to be 64 samples in length. The maximum number of orthogonal users that can exist in an FDMA or TDMA system with Nyquist sampling at 64 samples per bit duration is 64. We are especially interested in examining the 7-q constellations because the number of users exceeds 64.

[8] We briefly discuss DSSS to motivate the need for concurrent detector and waveform design. We leave quantitative comparison between our method and DSSS for later work.

[9] A fourfold reduction in computation relative to the same system using asynchronous DSSS is realized for our 6-3 constellation.

[10] We leave for future work the comparison of our WPMA joint detection system with other multiple access systems (DSSS, frequency hopped spread spectrum) using joint detection.

Table 1: Key to Figures 5, 7, and 6.

		matched filter	joint detector
constellation 7	64 users	———	———
constellation 7-2	66 users	+ · + · + · + ·	+ + + + + +
constellation 7-3	68 users	o · o · o · o · o	o o o o o o

In the 7 constellation (not shown), our WPMA scheme reduces, more or less, to FDMA for which $K = 64$. The 7-2 and 7-3 constellations (shown in Figure 4) allow 2 and 4 additional interfering users, respectively. Our scenarios consider a limited range of signal to noise ratios (SNR) in which the MAI is the limiting factor. Each constellation was run 1,000-2,000 times with different user bits for noise powers ranging from 0 to 0.63, i.e. $\sigma^2 = 0, \cdots, 0.63$. The bit detection was done with both a simple matched filter and the joint detection algorithm discussed in Section 3.

The BER is calculated from our simulations as the number of bits in error divided by the number of bits transmitted. The noise power, as shown in Equation 1, is σ^2, a single user's power is 1, and SNR $= 10log\frac{1}{\sigma^2}$. We present several BER versus SNR curves in Figures 5, 6, and 7. The key to the figures is shown in Table 4. These figures allow us to examine the performance degradation resulting from the addition of 2 and 4 correlated users to our orthogonal system (the 7 constellation) for both the matched filter and our joint detector. Hence, each figure shows the BER curve for the 7 constellation for which the joint detector and matched filter are identical.

Figure 5 shows the average BER for a user in each constellation. For high SNR, the matched filter is unable to overcome the MAI that results from the addition of 2 and 4 users to the 7 constellation whereas the WPMA joint detector offers only a small degree of degradation for each additional user pair. Overall, the WPMA joint detection system offers a substantial decrease in the BER over the matched filter system.

From the discussion in Section 3.2, we know that for our 7-q constellation, each user at level 7 has only one interferer (the user which is located above it in level q) while each user at level q has many interferes. Since a user at the lowest level and a user at the highest level of our constellations are dissimilar, we are curious to see the BERs experienced by users at both levels. We separate the BER curve for each constellation into two; one for the level 7 user and one for the level q user, where q = 2, 3. Figures 6 and 7 show the average BER of a user located at level q and level 7 of our constellations, respectively. From Figure 6, we see that the level 2 and level 3 user must endure BERs on the order of 17% for the matched filter; the joint detector, on the other hand, results in only minor performance degradation for the upper level users relative to the 7 constellation user.

We now turn our attention to Figure 7 for the level 7 user. Comparing the matched filter curves in Figures 6 and 7 confirms our predictions, namely, the matched filter detector gives us higher BERs for the level q user than for the level 7 user of the same constellation. The joint detector, however, gives us approximately the same BER for both the level 7 and level q user of the same constellation.

From these simulations and the ideas presented in this paper, we begin to see many opportunities for improving MA communications. One avenue that we shall pursue in future work is the development of smarter joint detection algorithms which exploit the hierarchical correlation structure of the wavelet packet waveform. In light of our simulation results, we expect smart detectors to further enhance system performance.

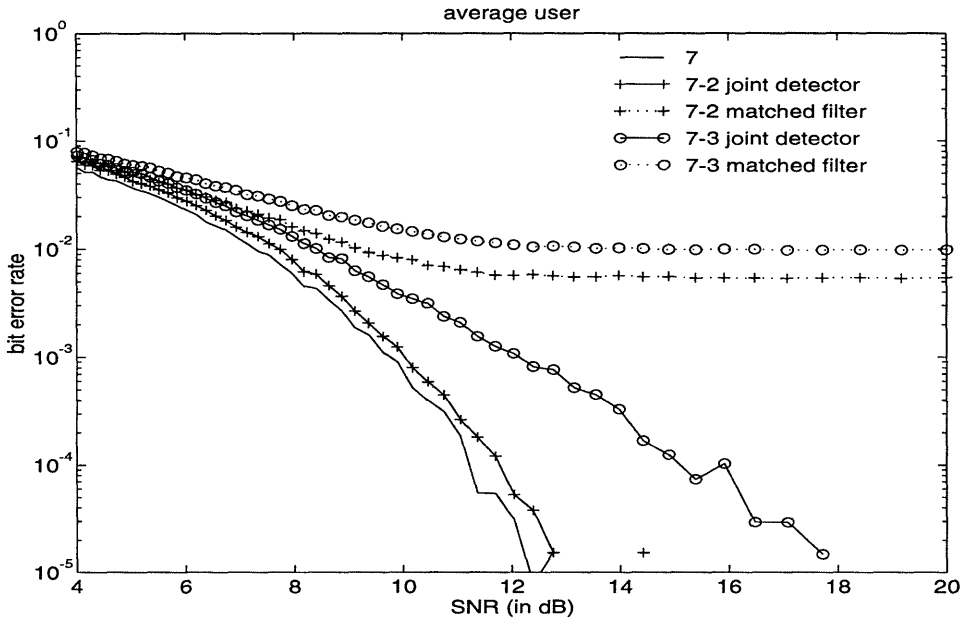

Figure 5: Average user bit error rate calculated from 64,000 to 136,000 simulated bit transmissions.

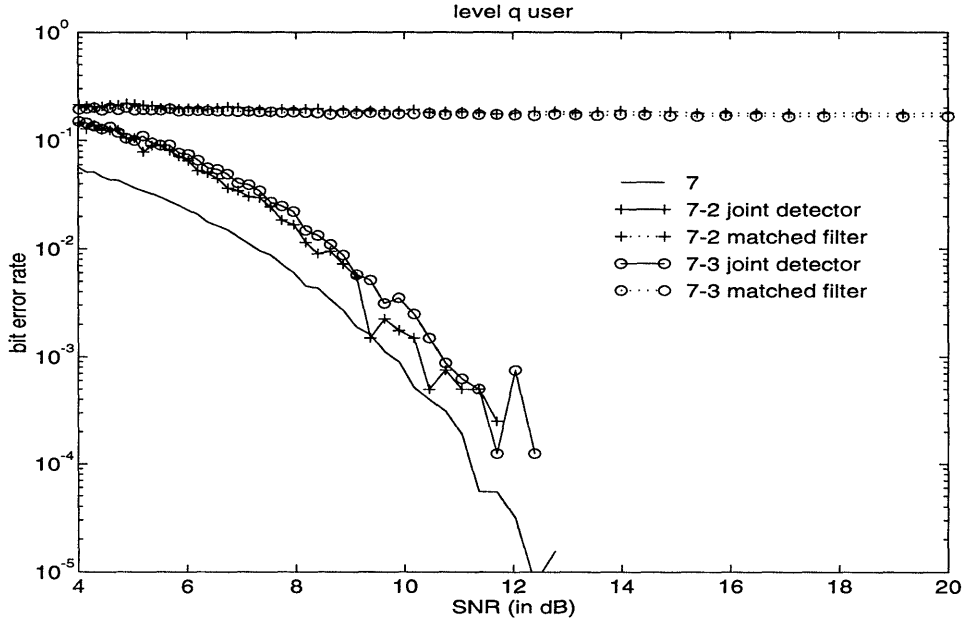

Figure 6: Level 2 and 3 user bit error rates are calculated from 2,000 to 8,000 bit transmissions. We note that due to the number of bit transmissions used for the calculation of these curves, the low bit error rate portion of these curves is not reliable and is presented here for completeness.

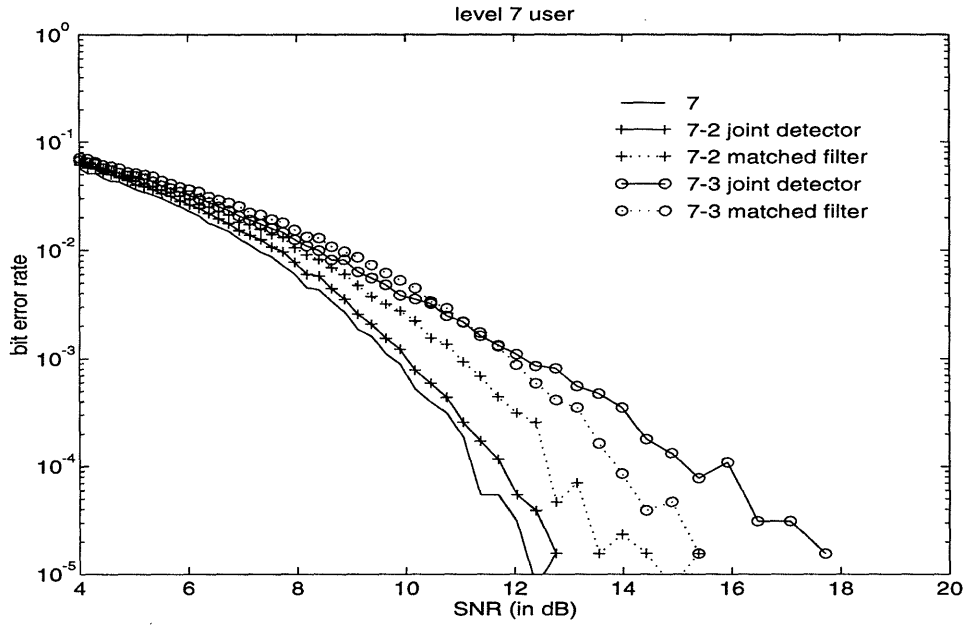

Figure 7: Level 7 user bit error rate calculated from 64,000 to 128,000 simulated bit transmissions .

5 FUTURE WORK

The joint detector of equation (17) will result in a cyclic behavior for many partially correlated user waveform sets. In our future work, we study the convergence of (17) and, as a result, enhance its robustness by a judicious modification of the symbol detection criterion. We also develop sufficient conditions for the algorithm to converge with a given waveform set (i.e. avoid oscillatory behavior of the estimates).

The p-q constellation discussed in this paper is just a first step in our analysis of the WPMA system. Wavelet packet constellations show much promise as they are naturally fraught with the versatility of providing the option for accommodating the varying nature of individual user's communication and processing needs. For example, within our WPMA constellation we may accommodate users with different transmission rates by allowing a single user to transmit multiple pulses within a single bin. We may also accommodate infrequent users by allowing them to cycle in and out of the system with the aid of a bin reserved for system control. WPMA systems are also suited for anti-jam communication through strategies such as bin hopping. The wavelet packet tableau may also serve as design tool for a single user who wishes to communicate at very high rates.

The simulations of the previous section along with the discussion in Section 3.2 enables us insight into the constellation design procedure. The wavelet packet constellation allows for simple visualization of the interaction of users and the strategic placement of users within the constellation. We may find that some users have computation constraints and some do not. For example, some users may be operating from a portable transmitter/receiver (limited in power and memory for computations) and others may use a fixed station. We see two ways of accommodating the portable user. We could assign this user to a small group so that number of bits which must be jointly detected is as small as possible. Alternatively, if a p-q constellation is used, the computationally simple matched filter detector results in only a small degradation in performance for the lowest level user, hence, we can place a computationally constrained user accordingly.

6 CONCLUSION

We have begun our exploration of the role that the wavelet packet transform can play to increase multiple access communication throughput and decrease receiver computational complexity. The work of the authors is focussed on combining waveform design with detection algorithm development to achieve MA systems that prevail over MA systems in which the receivers were designed independently of the waveforms. In this paper, we motivate the marriage of WPMA constellation design with receiver design to take advantage of the hierarchical nature of our wavelet packet signal sets. We offer a preliminary analysis and simulation results which indicate the potential for a marked computational improvement over the optimal detector, increased system performance over the matched filter detector, and additional flexibility and efficiency over other joint detection schemes for multiple access communication. We described a method for designing our wavelet-packet-based user waveforms and we discuss the nature of the cross correlation structure. We have focussed on a specific type of wavelet packet multiple access (WPMA) user constellation. Through simulations, we have shown that the addition of users to a saturated orthogonal system has little effect on system performance. For near zero noise, our WPMA joint detection system eliminates MAI. In general, the performance of our WPMA system is greatly enhanced by using a joint detector in place of a matched filter.

7 ACKNOWLEDGMENTS

This work was supported in part by the National Science Foundation under grant number MIP-9015281 and by the Air Force Office of Scientific Research under grant number F49620-92-J-0002. Dr. Claus is a visiting scientist supported by a research fellowship of the Deutsche Forschungsgemeinschaft (DFG).

The authors also wish to thank Professors Mitchell Trott and Gregory Wornell of MIT for their ongoing involvement in this work.

References

[1] K. S. Schneider. Optimal detection of code division multiplexed signals. *IEEE Trans. Aerospace Electronic Systems*, AES-15:181–185, Jan. 1979.

[2] S. Verdú. Minimum probability of error for asynchronous gaussian multiple-access channels. *IEEE Trans. Inform. Theory*, 32:85–96, Jan. 1986.

[3] M. Varanasi and B. Aazhang. Multistage detection in asynchronous code-division multiple-access communications. *IEEE Trans. on Comm.*, 38, Apr. 1990.

[4] Lupas R. and S. Verdu. Linear multiuser detectors for synchronous code-division multiple-access channels. *IEEE Trans. Inform. Theory*, 35:123–136, Jan. 1989.

[5] Lupas R. and S. Verdu. Near-far resistance of multiuser detectors in asynchronous channels. *IEEE Trans. on Comm.*, 38:496–508, Apr. 1990.

[6] R. R. Coifman and M. V. Wickerhauser. Entropy-based algorithms for best basis selection. *IEEE Trans. Inform. Theory*, IT-38:713–718, Mar. 1992.